Jointly Complementary&Competitive Influence Maximization with Concurrent Ally-Boosting and Rival-Preventing

Qihao Shi[1,2], Wenjie Tian[2], Wujian Yang[1,*], Mengqi Xue[1,2], Can Wang[1,2], Minghui Wu[1]
[1]School of Computing and Computer Science, Zhejiang University City College, Hangzhou 310015, China
[2]College of Computer Science, Zhejiang University, Hangzhou 310027, China
{shiqihao321,22121069}@zju.edu.cn,yangwj@zucc.edu.cn,{mqxue,wcan}@zju.edu.cn,mhwu@zucc.edu.cn

ABSTRACT

In this paper, we propose a new influence spread model, namely, Complementary&Competitive Independent Cascade (C^2IC) model. C^2IC model generalizes three well known influence model, i.e., influence boosting (IB) model, campaign oblivious (CO)IC model and the IC-N (IC model with negative opinions) model. This is the first model that considers both complementary and competitive influence spread comprehensively under multi-agent environment. Correspondingly, we propose the Complementary&Competitive influence maximization (C^2IM) problem. Given an ally seed set and a rival seed set, the C^2IM problem aims to select a set of assistant nodes that can boost the ally spread and prevent the rival spread concurrently. We show the problem is NP-hard and can generalize the influence boosting problem and the influence blocking problem. With classifying the different cascade priorities into 4 cases by the monotonicity and submodularity (M&S) holding conditions, we design 4 algorithms respectively, with theoretical approximation bounds provided. We conduct extensive experiments on real social networks and the experimental results demonstrate the effectiveness of the proposed algorithms. We hope this work can inspire abundant future exploration for constructing more generalized influence models that help streamline the works of this area.

PVLDB Reference Format:
Qihao Shi[1,2], Wenjie Tian[2], Wujian Yang[1,*], Mengqi Xue[1,2], Can Wang[1,2], Minghui Wu[1]. Jointly Complementary&Competitive Influence Maximization with Concurrent Ally-Boosting and Rival-Preventing. PVLDB, (): XXX-XXX, .
doi:XX.XX/XXX.XX

1 INTRODUCTION

During the past several decades, the Influence maximization (IM) problem has been extensively explored. Given a specific influence spread model, the IM problem asks to find a small number of early adopters of a product, such that the expected number of total adoptions is maximized over a social network. There are abundant influence spread models proposed. Starting with single agent scenario, kempe et.al. [18] first mathematically propose the independent cascade (IC) model and linear threshold (LT) model. The IC model and LT model are simple and effective, with both empirical interpretability and theoretical properties, i.e., monotonicity and submodularity. Therefore, subsequent research works focus on modifying these two models for variety of application requirements, e.g., topic-aware influence model [2], delay and critical time based influence model [13], offline location-aware model [20], multi-round model with feedback collected adaptively [35],opinion-aware model [10, 15] and profit and cost aware model [1, 34, 36], etc.

The above works all follow the single agent framework [18]. In nowadays social influence applications, there inevitably come up with the coexistence of multiple agents. Therefore, recent works turn to model the interactive behaviors between multiple agents, mainly including competition and complementary. The competition models describe the exclusive relations among agents, which finds applications in competitive viral marketing campaigns [3], social rumor control [6, 39], or epidemic immunization [8] and so on. The complementary models describe the improvement of the influence cascades with each other, e.g., node-based influence boosting model [22], cascade-based comparative enhancement model [25], post and repost interaction model [32].

All the above influence spread models incrementally introduce parameters or entities into a basic model, such that the model can fit for a specific real application. Such application driven research efforts are effective. However, there are quite a number of application scenarios. Constructing a new model for each scenario is arduous. Witnessed numerous influence spread models, a natural question arises: *Is there a framework model that can unify a number of existing models?* If such a model exists, then a series of applications can be solved under a single model, without implementing and executing a different algorithm for each application scenario. In this paper, we try to take a step for model unification, which may help streamline the research in this space.

Actually, Kempe et. al., [18] are the first to do such unification work. They propose the *triggering* model that generalizes the IC model and LT model. Similarly, we in this paper propose the Complementary&Competitive IC model (C^2IC), which generalizes the influence boosting (IB) model [22] (complementary model), campaign oblivious (CO)IC model [6] (competitive model) and the IC-N [10] (independent cascade model with negative opinions) model (single agent model). By unifying the existing three models, the C^2IC model can find applications for rumor control, influence boosting and competitive viral marketing.

The C^2IC model assumes the existence of both an ally agent and a rival agent. It defines a new kind of node as assistant node. When the ally cascade reaches an assistant node, a boosting cascade will be triggered, which improves the ally influence spread. In contrast,

Proceedings of the VLDB Endowment, Vol. , No. ISSN 2150-8097.
doi:XX.XX/XXX.XX

*Corresponding author: yangwj@zucc.edu.cn.

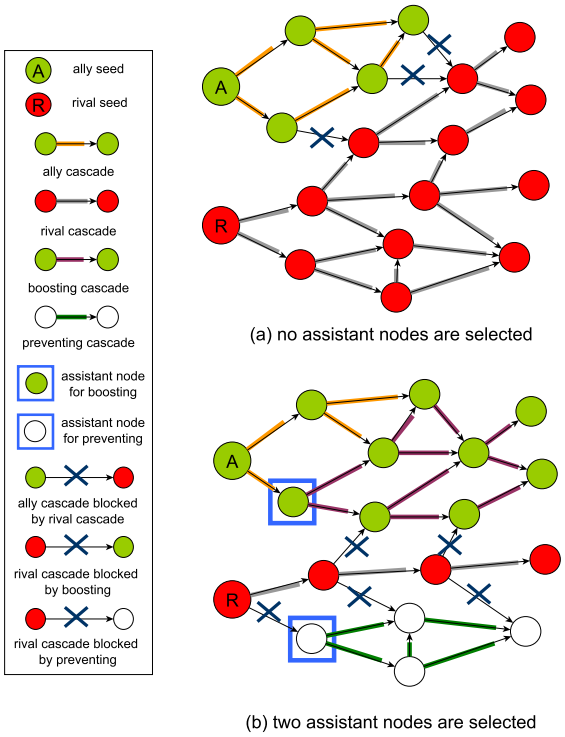

Figure 1: An example of C^2IC problem.

if the rival cascade reaches an assistant node, it also triggers a preventing cascade, which blocks the rival influence spread. We construct an example shown in Fig.1. Let node A be the ally seed, and node R be the rival seed. We can see if no assistant nodes are selected, the rival cascade spread fiercely, as shown in Fig.1(a). Note the ally cascade is blocked by the rival cascade if they reach the same node simultaneously, i.e., the rival cascade has higher priority than the ally cascade. However, if we select two assistant as shown in Fig.1(b), the ally cascade is boosted and the rival cascade is prevented considerably. Such results rely on a condition that both the preventing cascade and boosting cascade have higher priority than the rival cascade. A boosting cascade can be triggered from a user by attaching positive opinions to the ally information he receives. Similarly, a preventing cascade is triggered by attaching negative opinions of the rival information. In the example we can see, not only the network topology and seed node location, but also the priorities affect the influence spread significantly. Selecting appropriate assistant nodes can boost the ally cascade and prevent the rival cascade at the same time.

Easy to see that if only rival seed R exists, assistant node can only prevent the rival spread. Selecting assistant nodes that minimizes the rival cascade spread is exactly a rumor control instance under IC-N model [10]. If we constrain that no preventing cascade is triggered, it then becomes exactly the influence blocking problem [19]. Besides, if only ally seed A exists, assistant node can only boost the ally spread. Selecting assistant nodes that maximizes the ally cascade spread is an out-neighbor version of influence boosting instance [22]. The generalization of COIC model is implemented when multiple cascades reach the same node, the cascade with higher priority takes effect, see the blocked cases in Fig.1. Actually, if nodes are activated according to other particular rules when meeting multiple cascades, the C^2IC model can also generalize other multi-agent influence spread models. For example, if this node randomly choose one of the reaching cascade, the C^2IC model generalize the competitive IC model [3] as well.

In this paper, we try to take a step towards the unification work of influence spread models. This may help streamline the research works in this space. The main contributions are as follows.

- We propose the C^2IC model that generalizes the IB model, COIC model and the IC-N model. It describes the complex interactions of multiple cascades. Specifically, its reduction model C^+IC and C^-IC are specific versions of IB model and IC-N model respectively.
- We propose the C^2IM problem together with its reduced versions, i.e., C^+IM and C^-IM problems. We prove that all these three problems are NP-hard.
- Given different priorities, we conclude the monotonicity and submodularity holding conditions of different objective functions and classify the priorities into 4 M&S cases.
- We design efficient algorithms for solving the C^2IM problem under 4 M&S cases, with solid theoretical approximation guarantees and near linear time complexities provided. Specifically, we propose a tight submodular lower bound function that can be used for all non-submodular cases.
- We construct extensive experiments on 4 real datasets, with different settings of sample size and M&S cases. The results show the effectiveness of the proposed algorithms.

2 RELATED WORKS

The influence maximization (IM) problem was first studied for viral marketing by Domingos et al. [28]. The goal of the classic single agent IM problem is to choose a set S of "seed" nodes to adopt the product initially, such that the expected number of nodes adopting the product in the end is maximized [18]. A stochastic diffusion model is used to describe the dynamics of the influence propagation [12]. The IC model and the LT model are the two most popular ones [18]. Numerous variants of these two models are proposed by considering real world applications. To name some, time constrain models [13, 16] that introduce the influence spread delay and critical time, location-aware models [20, 30, 31] that consider the offline location context, topic-aware models [2, 9] that introduce topic models into influence spread, opinion-aware models [10, 15] that assume the users possess different opinions, adaptive or multi-round models [33, 35, 41, 44] that assume the influence spread results can be observed dynamically. These extensions all consider the single agent scenario.

By introducing multi agents scenario, another line of research works study the interaction behaviors between different cascades. As a common phenomenon, the competition attracts abundant research attention. In 2007, Bharathi et al. study the competitive IM problem with the opponents' strategies known beforehand [3]. Li et al. [21] study the case where the opponents' strategies are unknown, with Nash Equilibrium perspective. In 2010, Borodin et al. proposed a competitive LT model [4]. Another type of competition occurs when we are to minimize the spread of rumour [17, 45], which is known as rumor control. A common approach is to start

a competing campaign in the network, which is formally defined as the eventual influence limitation (EIL) problem [6]. A scalable algorithm is developed in [40] for EIL problem with near linear time complexity and nice approximation guarantees.

As we have mentioned, there are some works for noncompetitive multi agent scenarios. In 2012, Myers et al. [26] try to predict the probability of a user adopting a certain product given the results of previous influence spreads, where products have complementary relations. Similarly, Narayanam et al. [27] study the cross-sell between two sets of products. In 2015, Lu et al. [25] proposed the Comparative Independent Cascade (Com-IC) model to tackle the comparative multi-product influence maximization problem. The influence boosting model [22] further defines the improvement of an assistant that can boost the influence spread.

In this paper, we propose the C^{2}IC model which generalize a models from each of the above three cases. We hope this work can inspire abundant future exploration for constructing more generalized influence spread models.

3 INFLUENCE SPREAD MODEL

The social network is represented by $G = (V, E)$, where V is the node set and E is the edge set. Each edge e_{uv} has a probability p_{uv}. First we give the classic independent cascade (IC) model. Given a seed node set S, the IC model proceeds with discrete time steps. At time $t = 0$, nodes in S are activated. Then in each time $t > 0$, each node u that is newly activated at $t - 1$ will have a single chance to activate each of its inactive neighbor v, with the probability p_{uv}. The influence spread continues until no new node is activated. All active nodes remain active during the process.

3.1 The C^{2}IC Model

We propose the Complementary&Competitive IC model (C^{2}IC), which generalizes a more complicated real scenario. Specifically, in the C^{2}IC model, there are two cascades, i.e., ally cascade C_a and rival cascade C_r. We denote the nodes activated by cascade X as X-active. We define the assistant node set S, that can boost the ally cascade and prevent the rival cascade concurrently. In general, the influence spread of the two cascades follows the IC model themselves. The difference occurs when competition happens(multi cascades reach an assistant node), as below.

(1) **Ally boosting.** If C_a reaches an assistant node s, we denote the subsequent cascade originated from s as C_a^+. C_a^+ can successfully spread through an un-passed edge (u, v) with a probability of $p^+_{uv} \geq p_{uv}$.
(2) **Rival preventing.** If C_r reaches an assistant node s, we denote the subsequent cascade originated from s as C_r^-. C_r^- can successfully spread through an un-passed edge (u, v) with probability p_{uv}.
(3) **Competitive Spread.** When a node becomes X-active, it will not be activated by another cascade. When different cascades try to activate the same node, the cascade with higher priority dominates (discussed later).

The ally boosting property is extended from the boosted edge probabilities defined in the IB model [23]. The assistant nodes will start a boosted cascade that enhances the C_a-cascade by the boosted edge probabilities of all subsequent visited edges. Such enhancement is common in real influence spread scenarios that a user may attach additional positive information if she repost a tweet. The rival preventing property is inherited from IC-N model [11], where the assistant nodes will start an anti-spread with negative opinions against C_r cascade, after meeting C_r-cascade. The competitive spread property is inherited from the COIC model [7]. It models the exclusion of multiple competitive cascades. Obviously, the C^{2}IC model has two reduced versions.

- **C$^+$IC model:** Only cascade C_a and ally boosting exist. It is an out-neighbor version of the IB model, where C_a^+ spread through edges with the boosted probability.
- **C$^-$IC model:** Only cascade C_r and rival preventing exist. It is a special case of IC-N model, where the negative probabilities are 1 for assistant nodes and 0 for others.

3.2 Augmented Realization

The influence spread of a given seed set S' is usually represented by an expectation form using *realizations* of IC model. The generation of a *realization* is as follows.

Definition 1 (realization). *For each edge $(u, v) \in E$, flip a coin and denote it is "live" with probability of p_{uv}. After all coins flipped, take $L = (V, E')$ as a realization where V is the node set containing all nodes and E' is the edge set containing all "live" edges.*

Given a seed set S', define $\sigma(S')$ as the influence spread of S', i.e., the expected number of nodes that S' can activate. We have $\sigma(S') = \mathbb{E}[H(S', L)]$, where $H(S', L)$ is the number of nodes that S' can reach in L. Also we can write $\sigma(S') = \sum_{L \in \mathcal{L}} \Pr[L] H(S, L)$, where $\mathcal{L}$ is the space of all possible L and $\Pr[L]$ is the probability of generating L. Given the expectation form of influence spread, we define the *augmented realization (Aug-realization)* for C^{2}IC model.

Definition 2 (Aug-realization). *Given a realization L, for each edge $(u, v) \in E \backslash E'$, flipping a coin and denote it is "live-upon-boost" with probability $p^+_{uv} - p_{uv}$. After all coins flipped, taking $L^{aug} = (V, E'')$ as an Aug-realization where E'' contains all "live" and "live-upon-boost" edges.*

Given a randomly generated Aug-realization L^{aug}, we then can compute the number of reachable nodes by ally seed set S_a and rival seed set S_r. If the priority and assistant node set S is given, the status of all nodes are also definite in L^{aug}. Define $\sigma_a(S)$ and $\sigma_r(S)$ as the influence spread of the ally cascade and rival cascade with the assistant node set S, respectively. Note C_a^+-active nodes are also regarded as activated by C_a. These two variables can also be computed by the expectation of reachable node number in L^{aug}.

4 PROBLEM DEFINITION

Given the C^{2}IC model, we now define the jointly complementary and competitive influence maximization (C^{2}IM) problem. Define $f(S) = \sigma_a(S) - \sigma_a(\emptyset)$ as the increased number of C_a-active nodes and $g(S) = \sigma_r(\emptyset) - \sigma_r(S)$ as the reduced number of C_r-active nodes, by using assistant set S. The objective function of C^{2}IC problem is the weighted summation of function $f(S)$ and $g(S)$. Introducing a parameter $\lambda \in [0, 1]$, we have the objective function

$$h(S) = \lambda f(S) + (1 - \lambda) g(S).$$

Now given an ally seed set S_a and a rival seed set S_r, the C^{2}IM problem is formally defined as follows.

Problem 1 (C^{2}IM). *The C^{2}IM problem asks to select an assistant set S to maximize the weighted summation function:*

$$S^* = \arg\max_{S \subseteq V \setminus S_a \setminus S_r} h(S).$$

Naturally, we have two simplified versions of C^{2}IM problem by considering the C$^+$IC model and the C$^-$IC model.

Problem 2 (C$^+$IM). *The C$^+$IM problem asks to select an assistant set S to maximize the C_a-active increase function:*

$$S^* = \arg\max_{S \subseteq V \setminus S_a} f(S).$$

Problem 3 (C$^-$IM). *The C$^-$IM problem asks to select an assistant set S to maximize the C_r-active reduce function:*

$$S^* = \arg\max_{S \subseteq V \setminus S_r} g(S).$$

The following two theorems show the hardness of solving the above three problems and computing $f(S)$ and $g(S)$.

Theorem 1. *The three problems defined above are NP-hard.*

Proof. Consider the NP-hard problem of Maximum k-Coverage [42]. A Maximum k-Coverage instance consists of an integer k and a collection of m non-empty sets $C = \{c_1, c_2, ..., c_m\}$ with each C_i contains a set of elements $\{e_j\}$. It aims to find a subset $C' \subseteq C$ such that $|C'| \leq k$ and $|\cup_{c_i \in C'} c_i|$ is maximized. Next, we show the reduction from an arbitrary Maximum k-Coverage instance.

Let $G = \cup_{c_i \in C} c_i$ be the ground set. For each element e_j, we add e_j as a node into set V. For each set $c_i \in C$ that contains e_j, we add c_i as a node into set V, and add an edge (c_i, e_j) into set E. Now we obtain a graph $G = (V, E)$. Then we further add a node u, and connect u with each node c_i. Let E' be the set containing all edges out-going from u. Now we obtain a graph $G' = (\{u\} \cup V, E \cup E')$. Obviously, the above process can be performed in polynomial time.

Let all edges in E have a probability of 0, but boosted probability of 1. Let all edges in E' have a probability of 1. Let node u be the ally seed, then the C$^+$IM problem and the corresponding Maximum k-Coverage problem must have the same optimal solution. Let all edges have a probability of 1 and node u be the rival seed. The C$^-$IM problem and the corresponding Maximum k-Coverage problem must have the same optimal solution.

Further add a node v, and connect v with each node c_i. Let E'' be the set containing all edges out-going from v. Now we obtain a graph $G'' = (\{u\} \cup \{v\} \cup V, E \cup E' \cup E'')$. Let u be the ally seed and v be the rival seed. Let all edges in E have a probability of 0, but boosted probability of 1. Let all edges in E' and E'' have a probability of 1. Setting $\lambda = 1$ and $\lambda = 0$ corresponds to the C$^+$IM and C$^-$IM cases respectively, then the reduction from Maximum k-Coverage problem to C^{2}IM problem follows. □

Theorem 2. *Computing $f(\cdot)$ under C$^+$IC model is #P-hard, so is computing $g(\cdot)$ under C$^-$IC model.*

Proof. We can reduce the computing of $f(\cdot)$ and $g(\cdot)$ to the computing of influence spread [14], which is #P-hard. Now we add a node u and a node v and two edges (u, v),(v, s) with probabilities p_{uv} and p_{vs} into the graph. Further, let the boosted probability of (v, s) be $p^+_{vs} > p_{vs}$ while $p_e = p^+_e$ for all other edge e. If u is the ally seed, then $f(\{v\})$, is equal to the influence spread of s multiplied by $p^+_{vs} - p_{vs}$. Still consider the same graph. Let edge (u, v) and (v, s) both have a probability of 1. Let u be the rival seed. Then $g(\{v\})$ is equal to the influence spread of s added by 1. If we can compute $f(\{v\})$ or $g(\{v\})$, the influence spread of s can also be computed. Thus computing $f(\{v\})$ and $g(\{v\})$ is also #P-hard. □

Algorithm 1: PR-sketch-Generation(G, S_a, S_r, v)

```
Initialize a queue Q with only v in Q;
Initialize V^R = {v} and E^R = ∅;
while Q is not empty do
    t = Q.front();
    Q.pop_front();
    if t ∉ S_r ∪ S_a then
        for each incoming neighbour s of t do
            p = random(0, 1);
            if p > p^+_st then
                continue;
            else
                if p ≤ p_st then
                    Remark (s, t) as "live";
                else if p_st < p ≤ p^+_st then
                    Remark (s, t) as "live-upon-boost";
                Q.push_back(s);
                V^R = V^R ∪ {s};
                E^R = E^R ∪ {(s, t)};
return R = (V^R, E^R)
```

By similar reduction, we can see the objective function computation of C^{2}IM problem is also #P-hard when $\lambda = 1$ or $\lambda = 0$. Thus we may conclude that the computation of $f(\cdot)$ and $g(\cdot)$ under C^{2}IC model at least suffer the same hardness.

4.1 Partial Realization Sketch

Regarding the problem hardness, we introduce the well-known reverse influence sampling (RIS) [38] technique and construct a new data structure named partial realization (PR-)sketch, which the proposed sampling scheme builds upon.

Definition 3 (PR-sketch). *Given an ally set S_a, a rival set S_r, a root node v and a random generated augmented realization L^{aug}, a PR-sketch for v is the subgraph $R = (V^R, E^R)$, where V^R contains all nodes that can reach v in L^{aug} and E^R is the union of all the edges connecting nodes in V^R.*

Note a PR-sketch for v can be generated by a BFS process starting from v, with each edge (u, v) visited and remarked as "live" with probability p_{uv}, or "live-upon-boost" with probability of $p^+_{uv} - p_{uv}$. With probability $1 - p^+_{uv}$, we do not visit this edge. When no new node is visited, we end the BFS process and take all the nodes and edges visited to form a subgraph, which is the PR-sketch for v. The generation process is shown in Algorithm 1.

Define $gain(S, R)$ as the gain of selecting assistant node set S on PR-sketch R (gain computation discussed later). Suppose we sample a sizable set $\mathcal{R}$ of PR-sketch. Define $\Phi(S, \mathcal{R}) = \sum_{R \in \mathcal{R}} gain(S, R)$. Taking the expectation, we have

$$\mathbb{E}[gain(S, R)] = \mathbb{E}[\Phi(S, \mathcal{R})/|\mathcal{R}|] = \lambda f(S) + (1 - \lambda)g(S).$$

Thus we can estimate the value of objective function for any set S by sampling PR-sketches.

4.2 M&S Study with Priority Settings

The monotonicity and submodularity of the objective function is highly related to the priority of the cascades. In this subsection, we consider different priorities of the 4 cascades. We may analyze 4!=24 priorities, which contains up to 4 cases, i.e., monotone and submodular (M-S), monotone and non-submodular (M-nS), non-monotone and submodular (nM-S) and neither monotone nor submodular (nM-nS). For a set function h, we say it is monotone if $h(S \cup \{u\}) \geq h(S)$. We say it is submodular if $h(S \cup \{u\}) - h(S) \geq h(T \cup \{u\}) - h(T)$. All the M&S cases of priorities are listed in Table 1. We denote $X \succ X'$ if cascade X dominates X', i.e., if X and X' tries to activate a node at the same time, X takes effect.

Table 1: MS Properties under Different Priority Settings

M-S	nM-S
$C_a^+ \succ C_a \succ C_r^- \succ C_r$	
$C_a^+ \succ C_r^- \succ C_r \succ C_a$	
$C_r^- \succ C_r \succ C_a^+ \succ C_a$	
M-nS	**nM-nS**
$C_a^+ \succ C_a \succ C_r \succ C_r^-$	$C_a^+ \succ C_r^- \succ C_a \succ C_r$
$C_a \succ C_a^+ \succ C_r^- \succ C_r$	$C_r^- \succ C_a^+ \succ C_a \succ C_r$
$C_a \succ C_a^+ \succ C_r \succ C_r^-$	$C_r^- \succ C_a^+ \succ C_r \succ C_a$
$C_a^+ \succ C_r \succ C_r^- \succ C_a$	$C_r^- \succ C_a \succ C_a^+ \succ C_r$
$C_r \succ C_r^- \succ C_a^+ \succ C_a$	$C_r^- \succ C_a \succ C_r \succ C_a^+$
$C_r^- \succ C_r \succ C_a \succ C_a^+$	$C_a \succ C_r^- \succ C_a^+ \succ C_r$
$C_r \succ C_r^- \succ C_a \succ C_a^+$	$C_a \succ C_r^- \succ C_r \succ C_a^+$
$C_a^+ \succ C_r \succ C_a \succ C_r^-$	$C_a \succ C_r \succ C_r^- \succ C_a^+$
$C_r \succ C_a^+ \succ C_a \succ C_r^-$	$C_a \succ C_r \succ C_a^+ \succ C_r^-$
$C_r \succ C_a \succ C_a^+ \succ C_r^-$	$C_r \succ C_a \succ C_r^- \succ C_a^+$
$C_r \succ C_a^+ \succ C_r^- \succ C_a$	

Now we first show the priority conditions that affect the monotonicity of the objective function.

Lemma 1. *If $C_a \succ C_r \succ C_a^+$ or $C_a \succ C_r^- \succ C_a^+$ or $C_r^- \succ C_a^+ \succ C_r$ or $C_r^- \succ C_a \succ C_r$, the objective function $h(S)$ is not monotone. Otherwise, $h(S)$ is monotone.*

Proof. We know the objective function is not monotone if and only if adding an assistant node will decrease the objective value. In C^{2}IC model, the assistant node can only transform its descendants in the ways shown in Table 2 with the objective value changing. We only need to consider the decreasing cases.

Table 2: Objective Value Changing Transformation Cases

Increasing	Decreasing
$inactive \rightarrow C_a^+$	$C_a \rightarrow C_r, C_a \rightarrow C_r^-$
$C_r \rightarrow C_a, C_r \rightarrow C_a^+$	$C_a^+ \rightarrow C_r$
$C_r^- \rightarrow C_a^+$	

(1) $C_a \rightarrow C_r$. C_a^+ must be ordered after C_a and C_r. Accordingly, C_a^+ block the spread of C_a while itself will be blocked by C_r. Thus the patten $C_a \succ C_r \succ C_a^+$ must appear.

(2) $C_a \rightarrow C_r^-$. Similarly, one of its corresponding pattern is $C_a \succ C_r^- \succ C_a^+$ as C_a^+ can block C_a and be blocked by C_r^-. Additionally, another pattern for $C_a \rightarrow C_r^-$ is $C_r^- \succ C_a \succ C_r$. Note a node can be activated by C_r is also can be activated by C_r^-. Thus $C_a \succ C_r$ must appear. Otherwise, the transformation may become $C_r \rightarrow C_r^-$.

(3) $C_a^+ \rightarrow C_r^-$. The corresponding pattern is $C_r^- \succ C_a^+ \succ C_r$. Similarly, $C_a^+ \succ C_r$ must appear in this pattern. Otherwise, the transformation may become $C_r \rightarrow C_r^-$.

Therefore, we conclude that given a priority without the above 4 patterns, the objective function is monotone. □

For better illustrating Lemma 1, we construct an example in Fig.2. Let all the edges have a spread probability of 1. The counter examples are as follows.

(1) $S_a = \{A\}, S_r = \{E\}$ and $S = \{D\}$. The pattern $C_r^- \succ C_a \succ C_r$ implements the transformation of $C_a \rightarrow C_r^-$.
(2) $S_a = \{A\}, S_r = \{E\}$ and $S = \{B\}$. The pattern $C_a \succ C_r \succ C_a^+$ implements the transformation of $C_a \rightarrow C_r$.
(3) $S_a = \{A\}, S_r = \{E\}$ and $S = \{B, D\}$. The pattern $C_r^- \succ C_a^+ \succ C_r$ implements $C_a^+ \rightarrow C_r^-$ and the pattern $C_a \succ C_r^- \succ C_a^+$ implements $C_a \rightarrow C_r^-$.

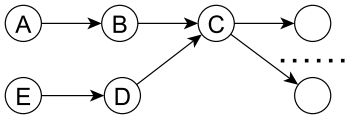

Figure 2: An example of Non-monotone cases.

Easy to check that the patterns in Lemma 1 cover all the nM cases in Table 1. Next we discuss the submodularity.

Lemma 2. *The objective function is submodular, if and only if the given priority satisfies the following two conditions simultaneously: (1) $C_r^- \succ C_r$ with no cascade ordered between them, (2) $C_a^+ \succ C_a$.*

Proof. If we select an assistant node that transforms a node from C_r to C_r^-, or transform a node from C_a to C_a^+, then all the descendants of this node perform the influence cascades of C_r^- or C_a^+. The submodularity can be proved by similar analysis according to the COIC model [7]. □

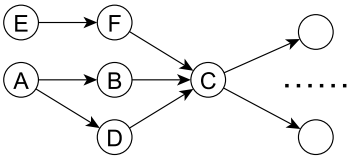

Figure 3: An example of Non-submodular cases.

We can also construct a counter example to show the nS cases, as illustrated in Fig.3. Let all the edge have a spread probability and boosted probability of 1. If $S_r = \{A\}$ and $C_r \succ C_r^-$, then selecting either B or D can only gain 1 as the rival spread still can reach C. However, selecting both B and D can make node C become C_r^--active. Thus if the pattern $C_r \succ C_r^-$ appears, the objective function is not submodular. In addition, if $C_r^+ \succ C_a \succ C_r$ and we further set $S_a = \{E\}$, we see that selecting either B or D will gain $-\lambda$. However, selecting D after B will gain 0, which violates the submodularity. Now let we constrain that the outgoing edges of C have a spread probability of 0, while boosted probability of 1. If $S_a = \{A\}$ and

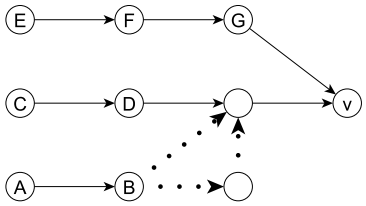

Figure 4: An example of gain computation on a PR-sketch

$C_a \succ C_a^+$, selecting either B or D can only gain 1 as the node C is C_a-active and its outgoing boosted influence spread cannot be triggered. We need to select both B and D that can trigger such boosted influence spread, which violates the submodularity.

We can see the above counter examples cover all the nS cases shown in Table 1, and the three M-S cases shown in Table 1 all satisfy the conditions discussed in Lemma 2.

4.3 GainComputation of PR-sketch

Given the priority, we then can present how to compute the gain of adding assistant node on a specific PR-sketch R for root v. Here we construct an example to better illustrate the gain computation. See in Fig.4. The solid lines are live edges and dashed lines are live-upon-boost edges. We show the GainComputation of selecting node s below. Note the gain is updated when one transformation of v in Table 2 appear in PR-sketch R. Otherwise, the gain is 0.

GainComputation(S_a, S_r, S, R)

(1) $inactive \rightarrow C_a^+$, $gain(s,R) = \lambda$.
(2) $C_a \rightarrow C_r^-$, $gain(s,R) = -1$.
(3) $C_a \rightarrow C_r$, $gain(s,R) = -1$.
(4) $C_r \rightarrow C_a^+$, $gain(s,R) = 1$.
(5) $C_r \rightarrow C_r^-$, $gain(s,R) = 1-\lambda$.
(6) $C_a^+ \rightarrow C_r^-$, $gain(s,R) = -\lambda$.
(7) $C_r^- \rightarrow C_a^+$, $gain(s,R) = \lambda$.

For all the cases in GainComputation, we can find an example in Fig.4 as follows.

(1) $S_a = \{A\}, S_r = \emptyset, S = \emptyset, s = B$.
(2) $S_a = \{C\}, S_r = \{E\}, S = \emptyset, s = F, (C_r^- \succ C_a \succ C_r)$.
(3) $S_a = \{C\}, S_r = \{E\}, S = \emptyset, s = D, (C_a \succ C_r \succ C_a^+)$.
(4) $S_a = \{A\}, S_r = \{C\}, S = \emptyset, s = B, (C_a^+ \succ C_r)$.
(5) $S_a = \emptyset, S_r = \{E\}, S = \emptyset, s = F$.
(6) $S_a = \{A\}, S_r = \{E\}, S = \{B\}, s = F, (C_r^- \succ C_a^+ \succ C_r)$.
(7) $S_a = \{A\}, S_r = \{E\}, S = \{B\}, s = F, (C_a^+ \succ C_r^- \succ C_r)$.
(8) **Zero gain example:** $S_a = \{E\}, S_r = S = \emptyset$, with any s.

5 PROBLEM SOLUTION

Since the objective function has 4 M&S cases given different priorities, we need to design 4 corresponding algorithms. All the proposed algorithms are based on PR-sketches. We first present the PR-IMM algorithm for the M-S case.

5.1 PR-IMM algorithm for M-S Case

Suppose we have already sampled a large number of PR-sketches $\mathcal{R} = \{R_i\}$ where $|\mathcal{R}| = \theta$ and $i \in [\theta]$. We then can select assistant nodes greedily. That is, selecting the node that brings largest marginal gain on $\Phi(S,\mathcal{R}) = \sum_{R\in\mathcal{R}} gain(S,R)$. In this section, we are considering the case that $h(S)$, accordingly $\Phi(S)$, is M-S. Hence a $(1-1/e)$-approximation ratio can be achieved by the greedy algorithm. For incorporating the PR-sketches, we utilize the sampling scheme proposed in the IMM method [37], which can ensure a $1-1/e-\varepsilon$ approximate solution with at least $1-\frac{1}{n^\ell}$ probability.

Algorithm 2: PR-IMM$(G, k, S_a, S_r, \ell, \varepsilon)$

1 Initial $\mathcal{R} = \emptyset$ and let $\ell' = \ell \cdot (1 + \log 2/\log n)$;
2 $\langle \mathcal{R}, \{\Psi(u)\}_{u\in V}\rangle$ =SampleGeneration$(G, k, \ell', \varepsilon)$;
3 S =GreedySelection$(S_a, S_r, \mathcal{R}, k, \{\Psi(u)\}_{u\in V})$;
4 **return** S

Generally, in the proposed PR-IMM algorithm (Algorithm 2), the SampleGeneration in Line 2 (Algorithm 3) is to sample a large enough PR-sketch set $\mathcal{R}$ and the GreedySelection in Line 3 (Algorithm 4) is to select a set S using $\mathcal{R}$. Let OPT be the maximum objective value obtained by optimal solution S^*. The parameters in Algorithm 2 and 3 are defined as

$$\alpha = \delta\sqrt{\ell \log n + \log 2}$$

$$\beta = \sqrt{\delta\left(\ell \log n + \log\binom{n}{k} + \log 2\right)}$$

$$\theta_i = (1 + \frac{\sqrt{2}}{3}\varepsilon) \cdot (\log\binom{n}{k} + \ell \log n + \log\log_2 n) \cdot \frac{2^i}{\varepsilon^2}$$

Note the $GainComputation(S_a, S_r, S, R)$ is implemented by enumerating the cases in Section IV.C for each node in R. By the IMM method [37], we have the following results.

Lemma 3. *If the GreedySelection returns an approximation for maximizing $\Phi(\cdot)$ with a ratio of δ, then with at least $1-n^{-\ell}$ probability, the set $\mathcal{R}$ returned by SampleGeneration satisfies*

$$|\mathcal{R}| \geq 2n_v(\alpha+\beta)^2\varepsilon^{-2}/OPT \quad \textit{(Theorem.2 in [37]).}$$

Meanwhile, given the above equation holds, with a probability of $1-n^{-\ell}$, GreedySelection returns a solution S satisfying

$$\lambda f(S) + (1-\lambda)g(S) \geq (\delta-\varepsilon)\cdot OPT \quad \textit{(Theorem.1 in [37]).}$$

We know that the greedy algorithm ensures $\delta = 1-1/e$ approximation ratio for the M&S function. Thus Algorithm 2 ensures a $1-1/e-\varepsilon$ approximate ratio.

Now we analyze the time complexity. Denote EPT as the expected complexity of generating one random PR-sketch. According to [37], the complexity of SampleGeneration is

$$O(\mathbb{E}[|\mathcal{R}|]\cdot EPT) = O\left(\frac{EPT}{OPT}(k+\ell)(n+m)\varepsilon^{-2}\log n\right).$$

Meanwhile, as a variation of the maximum coverage algorithm, Algorithm 4 (GreedySelection Algorithm) runs with a time complexity of $O\left(\sum_{R\in\mathcal{R}}|R|\right)$ [42], i.e., linear to the input size. Therefore, Algorithm 2 returns a $(1-1/e-\varepsilon)$-approximate solution with at least $1-2n^{-\ell'} = 1-n^{-\ell}$ probability. Together with the complexity analysis, we have the following theorem.

Theorem 3. *The PR-IMM algorithm returns a $(1-1/e-\varepsilon)$ approximate solution with at least $1-1/n^\ell$ probability. The time complexity is $O\left(\frac{EPT}{OPT}(k+\ell)(n+m)\varepsilon^{-2}\log n\right)$.*

Algorithm 3: SampleGeneration($G, k, S_a, S_r, \ell, \varepsilon$)

Initialize a set $\mathcal{R} = \emptyset$ and an integer $LB = 1$;
Initialize $\Psi(u) = 0$ for each $u \in V$;
for $i = 1$ *to* $\log_2 n - 1$ **do**
  for $j = |\mathcal{R}|$ *to* θ_i **do**
    R =PR-sketch-Generation(G, S_a, S_r, v);
    $\{\psi(u,R)\}_{u\in V}$ =GainComputation(S_a, S_r, R);
    $\forall u \in V, \Psi(u) = \Psi(u) + \psi(u,R)$;
    Insert PR-sketch R into $\mathcal{R}$;
  S = GreedySelection($S_a, S_r, \mathcal{R}, k, \{\Psi(u)\}_{u\in V}$);
  if $n \cdot \Phi(S,\mathcal{R}) \geq (1+\sqrt{2}\cdot\varepsilon)\cdot n/2^i$ **then**
    $LB = n \cdot \Phi(S,\mathcal{R})/(1+\sqrt{2}\cdot\varepsilon)$;
    break;
Compute $\theta = \frac{2n(\alpha+\beta)^2}{LB\cdot\varepsilon^2}$;
for $j = |\mathcal{R}|$ *to* θ **do**
  R =PR-sketch-Generation(G, S_a, S_r, v);
  $\{\psi(u,R)\}_{u\in V}$ =GainComputation(S_a, S_r, S, R);
  $\forall u \in V, \Psi(u) = \Psi(u) + \psi(u,R)$;
  Insert PR-sketch R into $\mathcal{R}$;
S = GreedySelection($S_a, S_r, \mathcal{R}, k, \{\Psi(u)\}_{u\in V}$);
return $\langle \mathcal{R}, \{\Psi(u)\}_{u\in V}\rangle$

Algorithm 4: GreedySelection($S_a, S_r, \mathcal{R}, k, \{\Psi(u)\}_{u\in V}$)

Initial $S = \emptyset$;
for $i = 1$ *to* k **do**
  $v = \arg\max_{v\in V\setminus S} \Psi(v)$;
  $S = S \cup \{v\}$;
  for *each PR-sketch* $R \in \mathcal{R}$ *that contains* v **do**
    $\{\phi(u,R)\}_{u\in R}$ = GainComputation(S_a, S_r, S, R);
    $\forall u \in R, \Psi(u) = \Psi(u) - \psi(u,R) + \phi(u,R)$;
return S

5.2 SA-IMM algorithm for M-nS Case

In this subsection, we will provide a data-dependent approximation algorithm for the M-nS case.

5.2.1 Sandwich Approximation Strategy. In the M-nS case, we can utilize the Sandwich Approximation (SA) Strategy [24] to find a data-dependent solution. Specifically, suppose we can find an upper bound function $U(S)$ and a lower bound function $L(S)$ of the objective function $h(S)$, where both $U(S)$ and $L(S)$ are submodular. Then we select three solution S_h, S_U and S_L greedily by maximizing $h(S)$, $U(S)$ and $L(S)$ respectively. Suppose S_U and S_L are $1-1/e-\varepsilon$ approximation solutions for maximizing $U(S)$ and $L(S)$. Let $S_{sa} = \arg\max_{S\in\{S_h,S_U,S_L\}} h(S)$. We have

$$h(S_{sa}) \geq \max\{\frac{L(S^*)}{h(S^*)}, \frac{h(S_U)}{U(S_U)}\}\cdot(1-1/e-\varepsilon)\cdot OPT,$$

See the effectiveness of SA strategy depends on how much $U(S)$ and $L(S)$ are close to the objective function $h(S)$. Thus the problem becomes how to derive $U(S)$ and $L(S)$ that are as close to $h(S)$ as possible while maintaining submodularity.

Here we can see the upper bound function $U(S)$ is easy to derive. Easy to check that any non-submodular priority can find an upper bound that is an M-S priority case in Table 1.

To derive a submodular lower bound function, we rewrite the objective function from a node-wise gain perspective. Let μ_{sv} denote the expected gain of node v if s is selected as an assistant node. Then by the independency of influence spread process [18, 43], we know that $h(\{s\}) = \sum_v \mu_{sv}$. Thus we have a lower bound function:

$$\underline{h}(S) = \sum_{v\in V} \max_{s\in S}\{\mu_{sv}\}.$$

Lemma 4. *The function $\underline{h}(S)$ is a lower bound function of $h(S)$ and it is monotone and submodular.*

Proof. Let $h(S,v)$ denote the expected gain of node v with assistant node set S. Obviously, we know that $h(S,v) \geq \mu_{sv}$ for any $s \in S$. Thus we have $h(S) = \sum_{v\in V} h(S,v) \geq \sum_{v\in V}\max_{s\in S}\mu_{sv} = \underline{h}(S)$. This proves that $\underline{h}(S)$ is a lower bound function of $h(S)$.

Next, $\underline{h}(S)$ is a simple summation of gain computation for each node once. For a specific node v, suppose the current maximal gain is achieved by assistant node s_1 in the current assistant node set S. Adding a new node s_2 into S either achieve a larger gain (i.e., $\mu_{s_2v} > \mu_{s_1v}$), or keep the same gain (i.e., $\mu_{s_2v} \leq \mu_{s_1v}$). Thus the monotonicity follows. Note in the former case, the marginal gain of adding s_2 is $\mu_{s_2v} - \mu_{s_1v}$, at least not larger than μ_{s_2v}. This holds true for any s_1, s_2 and S, which implies $\underline{h}(S\cup\{s_2\}) - \underline{h}(S) \geq \underline{h}(S\cup\{s_1,s_2\}) - \underline{h}(S\cup\{s_1\})$ that proves the submodularity. □

5.2.2 SA-IMM Algorithm. Given the submodular upper and lower bound functions, we are now ready to propose the sandwich approximation based (SA-)IMM algorithm, as shown in Algorithm 5. Lines 1-3 exactly follows the same process of PR-IMM algorithm (Algorithm 2). Here GreedySelectionUB function in line 3 is the GreedySelection algorithm (Algorithm 4), while the objective function is the upper bound function. In line 4, we greedily select the solution S_h on the same PR-sketch sampled in line 2, for maximizing the original objective function under the given priority setting. The difference is in lines 5-12 in Algorithm 5, where we give the process of selecting an approximate lower bound solution S_L.

For a fixed node v, we sample a set of PR-sketch $\mathcal{R}_v$. We do not know which s yield the maximum gain, thus we need to modify the sampling scheme so as to guarantee an error bound for each s. For any node s, we know $\mu_{sv} = \mathbb{E}[gain(s,R)]$. Let $F_v(s,\mathcal{R}_v) = \frac{\sum_{R\in\mathcal{R}_v} gain(s,R)}{|\mathcal{R}_v|}$. By similar analysis of RR sets [37], the PR-sketch sampling possesses the same martingale tail bounds. That is, given a set of randomly generated PR-sketches $\mathcal{R}_v$ with $\theta = |\mathcal{R}_v|$, for any node $v \in S$ and $\mu_{sv} = \mathbb{E}[gain(s,R)]$, we have

$$\Pr[\sum_{R\in\mathcal{R}_v} gain(s,R) - \theta\mu_{sv} \geq \delta\theta\mu_{sv}] \leq \exp(-\frac{\delta^2}{2+\frac{2}{3}\delta}\theta\mu_{sv}),$$

holds for any $\delta > 0$ and

$$\Pr[\sum_{R\in\mathcal{R}_v} gain(s,R) - \theta\mu_{sv} \leq -\delta\theta\mu_{sv}] \leq \exp(-\frac{\delta^2}{2}\theta\mu_{sv}),$$

Algorithm 5: SA-IMM($G, k, S_a, S_r, \ell, \varepsilon_1, \varepsilon_2$)

Initial $\mathcal{R} = \emptyset$ and let $\ell' = \ell \cdot (1 + \log 2/\log n)$;
$\langle \mathcal{R}, \{\Psi(u)\}_{u\in V}\rangle$ =SampleGeneration($G, k, \ell', \varepsilon_1$);
S_U =GreedySelectionUB($S_a, S_r, \mathcal{R}, k, \{\Psi(u)\}_{u\in V}$);
S_h =GreedySelection($S_a, S_r, \mathcal{R}, k, \{\Psi(u)\}_{u\in V}$);
$\kappa = \frac{\varepsilon_2}{2-\varepsilon_2}$;
$\theta = (2 + \frac{2}{3}\kappa)(2 - \frac{1}{e} + \kappa)\frac{(\ell+1)\log n + \log 2}{\kappa^3(3-\frac{1}{e})}$;
Initialize a set $\mathcal{R}_v = \emptyset$ for each node v;
for *each* $v \in V$ **do**
  for $j = 0$ *to* θ **do**
    R =PR-sketch-Generation(G, S_a, S_r, v);
    Insert PR-sketch R into $\mathcal{R}_v$;
S_L =GreedySelectionLB($S_a, S_r, \{\mathcal{R}_v\}_{v\in V}, k$);
return $\langle S_U, S_h, S_L\rangle$

holds for any $0 < \delta < 1$. Now, we show the error bound of estimating μ_{sv} for any s and v using PR-sketch set $\mathcal{R}_v$.

Lemma 5. *Given* $\mathcal{R}_v$ *that*

$$\theta = |\mathcal{R}_v| \geq (2 + \frac{2}{3}\kappa)\frac{(\ell+1)\log n + \log 2}{\gamma \cdot \kappa^2},$$

it holds $\forall s \in V$ *simultaneously with at least* $1 - \frac{1}{n^\ell}$ *probability*

$$\begin{aligned} &\text{if} \quad \mu_{sv} \geq \gamma, |\mu_{sv} - F_v(s, \mathcal{R}_v)| < \kappa\mu_{sv}, \\ &\text{if} \quad \mu_{sv} < \gamma, |\mu_{sv} - F_v(s, \mathcal{R}_v)| < \kappa\gamma. \end{aligned}$$

Proof. Fix a node s. We know that $\mu_{sv} = \mathbb{E}[gain(s, R)]$. Then $|\mathcal{R}_v| \cdot F_v(\mathcal{R}_v)$ can be regarded as $|\mathcal{R}_v|$ times of i.i.d. Bernoulli variables with a mean of μ_{sv}. If $\mu_{sv} < \gamma$, we have

$$\begin{aligned} &\Pr[|F_v(s, \mathcal{R}_v) - \mu_{sv}| \geq \kappa\gamma] \\ &= \Pr[\sum_{R\in\mathcal{R}_v} gain(s, R) - \theta\mu_{sv} \geq \theta\frac{\kappa\gamma}{\mu_{sv}}\mu_{sv}] \\ &\leq 2\exp(-\frac{\frac{\kappa^2\gamma^2}{\mu_{sv}}}{2 + \frac{2\kappa\gamma}{3\mu_{sv}}}|\mathcal{R}_v|) = 2\exp(-\frac{3\kappa^2\gamma^2}{6\mu_{sv} + 2\kappa\gamma}\theta) \\ &< 2\exp(-\frac{3\kappa^2\gamma^2}{6\gamma + 2\kappa\gamma}\theta) = \frac{1}{n^{\ell+1}}. \end{aligned}$$

Meanwhile, if $\mu_{sv} \geq \gamma$, then we have

$$\begin{aligned} &\Pr[|F_v(s, \mathcal{R}_v) - \mu_{sv}| \geq \kappa\mu_{sv}] \\ &= \Pr[\sum_{R\in\mathcal{R}_v} gain(s, R) - \theta\mu_{sv} \geq \theta\kappa\mu_{sv}] \\ &\leq 2\exp(-\frac{\kappa^2\mu_{sv}}{2 + \frac{2}{3}\kappa}\theta) \leq \frac{1}{n^{\ell+1}}. \end{aligned}$$

Taking the union bound, the lemma is proved. □

Suppose S is the solution returned by GreedySelectionLB function. Define set $V_\gamma = \{v | \max_{s\in S}\{\mu_{sv}\} \geq \gamma\}$. Given Lemma 5 holds, then we have

$$\begin{aligned} &\underline{h}(S) = \sum_{v\in V}\max_{s\in S}\{\mu_{sv}\} = \sum_{v\in V_\gamma}\mu_{sv} + \sum_{v\in V\setminus V_\gamma}\mu_{sv} \\ &\geq \sum_{v\in V_\gamma}\frac{F_v(S, \mathcal{R}_v)}{1+\kappa} + \sum_{v\in V\setminus V_\gamma}(F_v(S, \mathcal{R}_v) - \kappa\gamma) \\ &\geq \sum_{v\in V}\frac{F(S, \mathcal{R}_v)}{1+\kappa} - n\kappa\gamma \geq \frac{1-1/e}{1+\kappa}\sum_{v\in V}F(S^*, \mathcal{R}_v) - n\kappa\gamma \\ &\geq \frac{1-1/e}{1+\kappa}(\sum_{v\in V_\gamma}(1-\kappa)h(S^*) + \sum_{v\in V\setminus V_\gamma}(h(S^*) - \kappa\gamma)) - n\kappa\gamma \\ &= (1 - \frac{1}{e})\frac{1-\kappa}{1+\kappa}OPT - (\frac{1-1/e}{1+\kappa} + 1)n\kappa\gamma \end{aligned}$$

See the approximation guarantee and the sampling number are both controlled by parameters κ and γ. By setting $\gamma = \frac{\gamma'}{n}OPT$, and setting κ to the value that satisfies $(1+\kappa)\varepsilon_2 = 2\kappa + (2 - \frac{1}{e} + \kappa)\gamma'\kappa$. We can make the approximation guarantee become a nice formulation, i.e., $\underline{h}(S) \geq (1 - \frac{1}{e} - \varepsilon_2)OPT$.

By utilizing similar lower bound estimation method of IMM [37], we can get a lower bound of OPT, so as to further get a definite value of γ that can make the above guarantee holds. However, such setting may lead the sampling number dominated by a factor of n for each node v, which makes the total sampling number dominated by a factor of n^2.

Therefore, we consider a simple case by artificially setting $\kappa = \frac{\varepsilon_2}{2(1-1/e))-\varepsilon_2}$. With $\kappa \in (0, 1]$, we have $\varepsilon \in (0, 1 - \frac{1}{e}]$ and

$$\underline{h}(S) \geq (1 - \frac{1}{e} - \varepsilon_2)OPT - (\frac{1-1/e}{1+\kappa} + 1)n\kappa\gamma.$$

We further set $\gamma = \frac{\kappa(3-1/e)}{(2-1/e+\kappa)}$. Then we have $\gamma \in (0, 1]$ and

$$\underline{h}(S) \geq (1 - \frac{1}{e} - \varepsilon_2)OPT - \frac{(3-1/e)\kappa^2}{1+\kappa}n.$$

The sampling number is then

$$\theta = |\mathcal{R}_v| = (2 + \frac{2}{3}\kappa)(2 - \frac{1}{e} + \kappa)\frac{(\ell+1)\log n + \log 2}{\kappa^3(3-1/e)},$$

Replacing κ by $\frac{\varepsilon_2}{2-\varepsilon_2}$, the total time complexity for selecting the solution for lower bound function is then $O(EPTn\ell\varepsilon_2^{-3}\log n)$. Now, we have the following result.

Theorem 4. *For any* $\varepsilon_1 > 0, \varepsilon_2 \in (0, 1-\frac{1}{e}]$ *and* $\kappa = \frac{\varepsilon_2}{2(1-1/e))-\varepsilon_2}$, *with at least* $1 - 2/n^\ell$ *probability, the SA-IMM algorithm (Algorithm 5) returns a solution* S_{sa} *satisfies the following two data-dependent approximation guarantees:*

$$\begin{aligned} h(S_{sa}) &\geq \frac{h(S_U)}{U(S_U)} \cdot (1 - 1/e - \varepsilon_1) \cdot OPT, \\ h(S_{sa}) &\geq \frac{L(S^*)}{h(S^*)} \cdot (1 - 1/e - \varepsilon_2) \cdot OPT - \frac{(3-1/e)\kappa^2}{1+\kappa}n. \end{aligned}$$

The time complexity is $O(\max\{T_1, T_2\})$, *where* $T_1 = \frac{EPT}{OPT}(k + \ell)(n + m)\varepsilon_1^{-2}\log n$ *and* $T_2 = EPTn\ell\varepsilon_2^{-3}\log n$).

Remark. *In Algorithm 5, we see* $\kappa\gamma = \frac{\kappa^2(3-1/e)}{(2-1/e+\kappa)}$. *When* $\kappa = 1$, $\gamma = 1$, *Lemma 5 holds with the case that* $h(s, v) \leq \gamma = 1$. *When* $\kappa = 0$, $\gamma = 0$ *and* $\kappa\gamma = 0$, *for all* $h(s, v) \geq \gamma = 0$, *we need to sample infinity*

Algorithm 6: RG-IMM$(G, k, S_a, S_r, \ell, \varepsilon)$

Initial $\mathcal{R} = \emptyset$ and let $\ell' = \ell \cdot (1 + \log 2/\log n)$;
$\langle \mathcal{R}, \{\Psi(u)\}_{u\in V}\rangle$ =SampleGeneration$(G, k, \ell', \varepsilon)$;
S =RandomGreedy$(S_a, S_r, \mathcal{R}, k, \{\Psi(u)\}_{u\in V})$;
return S

Algorithm 7: RandomGreedy$(S_a, S_r, \mathcal{R}, k, \{\Psi(u)\}_{u\in V})$

Initial $S = \emptyset$ and $S_0 = \emptyset$;
for $i = 1$ *to* k **do**
  $\forall u \in V, \Psi'(u) = \Psi(u)$;
  for *each* $R \in \mathcal{R}$ *that contains a node in* S_{i-1} **do**
    $\{\phi(u, R)\}_{u\in V}$ = GainUpdate(S_a, S_r, S_{i-1}, R);
    $\forall u \in V, \Psi'(u) = \Psi'(u) - \psi(u, R) + \phi(u, R)$;
  Initial $S_i = \emptyset$;
  for $j = 1$ *to* k **do**
    $v = \arg\max_{v\in V\setminus\{S_i\cup S_{i-1}\}} \Psi'(v)$;
    $S_i = S_i \cup \{v\}$;
  Select a node u uniformly at random from S_i;
  $S = S \cup \{u\}$;
return S

PR-sketches to ensure zero error of all $h(s, v)$. With ε_2 being small, the absolute error factor $\frac{\varepsilon_2^2(3-1/e)}{2(2-\varepsilon_2)}$ correspondingly become small. In real applications, we can tune an appropriate value of ε_2 to balance the trade-off between performance and running time.

5.3 RG-IMM algorithm for nM Cases

We first consider the nM-S case. By replacing the GreedySelection function in PR-IMM algorithm (Algorithm 2) by the RandomGreedy Algorithm [5] (shown in Algorithm 7), we can achieve a $(\frac{1}{e} - \varepsilon)$-approximate solution. The corresponding RG-IMM algorithm is shown in Algorithm 6. It is proved in [5] that the RandomGreedy algorithm can guarantee a $\frac{1}{e}$-approximate solution for maximization problem of non-monotone submodular function. Similar to Theorem 3, by replacing δ with $\frac{1}{e}$ in Lemma 3, we can show the performance guarantee of RG-IMM Algorithm as follows.

Theorem 5. *The RG-IMM algorithm (Algorithm 6) returns a $(1/e - \varepsilon)$-approximate solution with at least $1 - 1/n^\ell$ probability. The time complexity is $O\left(\frac{EPT}{OPT}(k + \ell)(n + m)\varepsilon^{-2}\log n\right)$.*

SA-RG-IMM algorithm for the nM-nS case. Similarly, we can replace all the GreedySelection functions (including GreedySelectionUB and GreedySelectionLB) by RandomGreedy algorithm. With all other steps the same to SA-IMM algorithm (Algorithm 5), we can derive an algorithm for the nM-nS case, which is named as SA-RG-IMM algorithm. Similar to Theorem 4, we have the following results by setting $\gamma = \frac{\kappa(2+1/e)}{1+1/e+\kappa}$ and $\kappa = \frac{\varepsilon_2}{2/e-\varepsilon_2}$.

Theorem 6. *For any $\varepsilon_1 > 0$, $\varepsilon_2 \in (0, \frac{1}{e}]$ and $\kappa = \frac{\varepsilon_2}{2/e-\varepsilon_2}$, with at least $1 - 2/n^\ell$ probability, The SA-RG-IMM algorithm returns a solution S_{sa} satisfies the following two data-dependent approximation guarantee:*

$$h(S_{sa}) \geq \frac{h(S_U)}{U(S_U)} \cdot (1/e - \varepsilon_1) \cdot OPT,$$
$$h(S_{sa}) \geq \frac{L(S^*)}{h(S^*)} \cdot (1/e - \varepsilon_2) \cdot OPT - \frac{(2 + 1/e)\kappa^2}{1 + \kappa} n.$$

The time complexity is $O(\max\{T_1, T_2\})$, where $T_1 = \frac{EPT}{OPT}(k + \ell)(n + m)\varepsilon_1^{-2}\log n$ and $T_2 = EPTn\ell\varepsilon_2^{-3}\log n$).

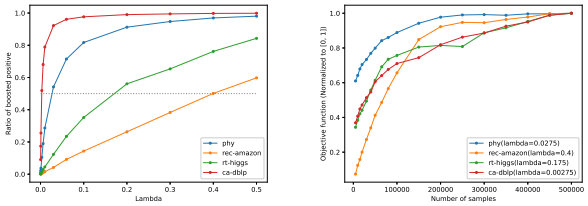

(a) Ratio of boosted C_a (b) Objective value changing

Figure 5: PR-IMM test with λ and sample size varying

6 EXPERIMENTS

6.1 Experimental Settings

6.1.1 Datasets. We use four public available real-world networks. **(1) Phy** [14]. This dataset is extracted from Physics section, representing the coauthor relations. It has 37.2K nodes and 174.2K undirected edges. **(2) rec-Amazon** [29]. The network was collected from Amazon website, representing the co-purchase relations between products. It has 91.8K nodes and 125.7K undirected edges. **(3) rt-Higgs** [29]. This is a retweet networks, representing the retweet relation between users. It has 425K nodes and 733.6K undirected edges. **(4) ca-DBLP** [29]. DBLP is a widely used collaboration networks representing co-author relationships. It has 317.1K nodes and 1.1M undirected edges. In the experiments, we change each undirected edge to a bi-directed edge.

6.1.2 Parameters and Measurements. .

Edge probabilities. For a node v, we set the spread probability of each incoming edge of v to $\frac{1}{d_v}$, where d_v is the incoming degree of node v. The boosted probability of edge (u, v) is $1 - (1 - p_{uv})^2$ following the setting of IB model [23], where p_{uv} is the spread probability of edge (u, v).

Seed nodes. For each datasets, we first extract the top 25% degree nodes. Then we randomly and uniformly select m nodes as the ally seed set S_a and m nodes as the rival seed set S_r respectively. Here we set $m = N/1000$ where N is the total number of nodes.

Priorities. We select three priorities to test the performance of the proposed algorithms, i.e., $C_a^+ \succ C_r^- \succ C_r \succ C_a$ for PR-IMM, $C_a \succ C_a^+ \succ C_r^- \succ C_r$ for SA-IMM and $C_a^+ \succ C_r^- \succ C_a \succ C_r$ for SA-RG-IMM respectively. The upper bound function of SA-IMM and SA-RG-IMM are the objective functions with priority $C_a^+ \succ C_r^- \succ C_r \succ C_a$ as well. Note there is no nM-S case priority exists, so we do not implement the RG-IMM experiments.

Evaluations. We use the objective value as the performance metrics. The value is measured by taking the average over 10000 times of Monte Carlo simulations given the solution assistant set.

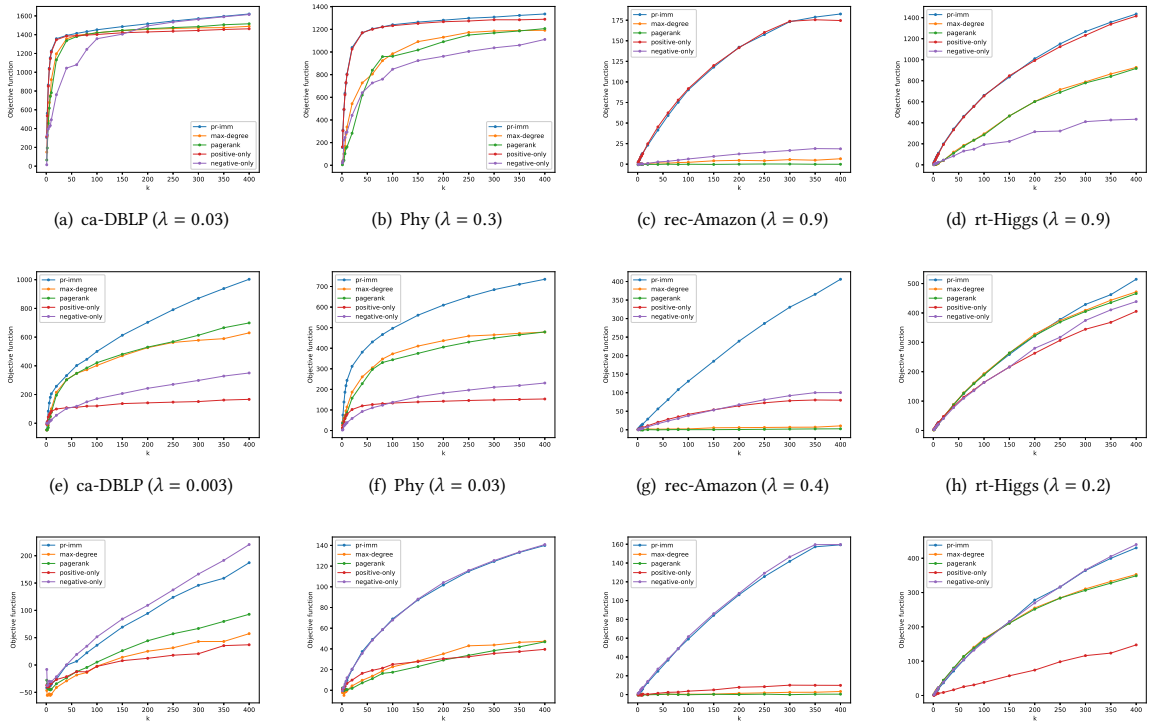

(a) ca-DBLP ($\lambda = 0.03$) (b) Phy ($\lambda = 0.3$) (c) rec-Amazon ($\lambda = 0.9$) (d) rt-Higgs ($\lambda = 0.9$)

(e) ca-DBLP ($\lambda = 0.003$) (f) Phy ($\lambda = 0.03$) (g) rec-Amazon ($\lambda = 0.4$) (h) rt-Higgs ($\lambda = 0.2$)

(i) ca-DBLP ($\lambda = 0.0003$) (j) Phy ($\lambda = 0.003$) (k) rec-Amazon ($\lambda = 0.04$) (l) rt-Higgs ($\lambda = 0.02$)

Figure 6: Performance of PR-IMM with Different λ Value with k Varying.

In the experiments, we vary λ, k and sample times respectively to observe the performance changing.

6.1.3 Comparison algorithms. In this paper, we test the performance of PR-IMM, SA-IMM and SA-RG-IMM algorithms under different priorities. Note the positive-only and negative-only comparisons also have upper bound and lower bound versions for SA-IMM and SA-RG-IMM algorithms. The comparison methods include: **(1) max-degree:** Selecting the top-k nodes with the maximum summation of in-degree and out-degree. **(2) pagerank:** Selecting the top-k ranked nodes with the well-known pagerank algorithm. **(3) positive-only:** The proposed algorithm in this paper, that only consider ally boosting. **(4) negative-only:** The proposed algorithm in this paper, that only consider rival preventing.

6.2 Results of PR-IMM under M-S case

6.2.1 Test by varying λ and sample size. We first vary the parameter λ and the sample size, to observe the objective function value changing. First, we fix the sample number to 100K, the assistant set size to 400 and tune λ. Given the returned solution set S, the C_a cascade boosting ratio is $\lambda f(S)/h(S)$. It measures the hardness of ally boosting compared with rival preventing. The results are shown in Fig.5(a). For the 4 datasets, λ becomes large means we pay more attention on ally boosting. Correspondingly, the C_a boosting ratio first increase rapidly while slows down after an inflection point. A sharp increase of C_a boosting ratio means the selected assistant node can trigger powerful C_a^+ cascade. The increase of the objective function mainly relies on the ally boosting. As we can see, the dataset densities of ca-DBLP and Phy are much higher than that of rec-Amazon and rt-Higgs. This is consistent to the results in Fig.5(a), since a denser network has higher competition probability between C_a and C_r cascades. The C_a^+ cascade can also block the C_r cascade, which makes the boost operation yield larger gain.

To show the performance changing with varying of sample numbers, we fix the λ value near inflection points (shown in the legend) in Fig.5(a), and present the changing of objective value in Fig.5(b). The objective function value is normalized by the maximum objective value obtained among all cases of sample size. We can see the objective value of all the datasets tends to be stable when sample size reach 150K. In the following, we fix sample size to 150K.

6.2.2 Performance with different λ. For each datasets, we set three different λ value to further observe the performance with assistant set size k varied. We constrain the value of λ to be large, middle and small respectively (shown in the captions in subgraphs of Fig.6). The results are shown in Fig.6. In all the datasets, we can see, with large λ (results in Fig.6(a-d)), PR-IMM and the positive-only methods are most outperforming. While with small λ (results in Fig.6(i-l)), PR-IMM and the negative-only methods are most outperforming. This is consistent to the expectation since large λ and small λ makes the PR-IMM better focus on the ally boosting and rival preventing respectively. Accordingly, with middle λ, only the PR-IMM algorithm performs well, while both the positive-only and negative-only performs poor. This demonstrates the effectiveness of the proposed PR-IMM algorithms, where both the ally-boosting and rival-preventing are balanced. In addition, positive-only and

negative-only are indeed special cases of PR-IMM. Therefore, we can conclude that the PR-IMM algorithm is practical for dealing with variety of influence control applications, by tuning the parameter λ flexibly.

6.3 Results of SA-IMM under M-nS case

6.3.1 Test by varying λ and sample size. Similarly, we first show the affection of parameter λ and sample size. In Fig.7(a), we can see similar phenomenon as that in Fig.5(a). The affection of λ is highly related to the network topology and density. We show in Fig.7(b) and (c), the changing of objective function varying the sample number for upper bound function and for lower bound function, with $\lambda = 0.027$ for Phy, 0.5 for rec-Amazon and 0.33 for rt-Higgs respectively, according to the inflection point in Fig.7(a). Fig.7(b) is very similar to that in Fig.5(b), thus we fix the sample size of upper bound optimization to 150K. In Fig.7(c), we can see the objective value of all the datasets tends to be stable when sample size is larger than 5. Thus in lower bound optimization of SA-IMM, we fix sample size to 5 per node.

6.3.2 Performance with different λ. For each datasets, we set three different λ value to further observe the performance with assistant set size k varied. We constrain the value of λ to be large, middle and small respectively (shown in the captions in subgraphs of Fig.8). The results are shown in Fig.8. The results of SA-IMM algorithm are more complex than that of PR-IMM, since we conduct the upper bound and lower bound optimization for all the SA-IMM, positive-only and negative-only methods respectively.

In all the cases of the three datasets, we can see, at least one of the SA-IMM-upper and SA-IMM-lower performs the best among all the comparisons. In addition, we observe that each of these two methods outperforms the other in several cases, with quite small gaps. Thus we can conclude that the upper bound and lower bound optimization of SA-IMM are both effective. More specifically, the upper bound optimization is more effective if λ is large. As the upper bound we use in this paper adopt the priority $C_a^+ \succ C_r^- \succ C_r \succ C_a$. When λ is large, we are more interested in ally boosting, which is strongly supported by C_a^+ cascade that having the highest priority. In contrast, when λ is small, the lower bound optimization is more effective, since the algorithm focus on rival preventing and C^- has the second highest priority.

Similarly to the results in Fig.6, the lower and upper bound based on positive-only methods exhibit comparable performance to the two SA-IMM methods, when λ is large in Fig.8(a-c). The lower and upper bound based on negative-only methods exhibit comparable performance to the two SA-IMM methods, when λ is small in Fig.8(g-i). These phenomena are consistent to the fact that large λ better support ally boosting while small λ support rival preventing more strongly. When λ takes the middle value, the two SA-IMM methods are much more outperforming than the positive-only and negative-only methods. All the results demonstrate the effectiveness of the proposed SA-IMM algorithm.

An exception is the result in Fig.8(f). The max-degree and pagerank methods perform quite well. This is due to the special topology of rt-Higgs dataset. It is a sparse dataset with low density. Meanwhile, its diagram is larger than other datasets. This makes the selected seed nodes for ally and rival very scattered. With middle valued λ, the SA-IMM algorithm may perform poorly as the seed nodes can hardly share the same assistant nodes. However, the largest node degree in rt-Higgs is 30K. Such high degree nodes can be easily caught by max-degree and pagerank algorithms, which indeed is a good choice to serve as an assistant node. Thus if a dataset is sparse but having very high degree center nodes, simple algorithms may be better choices, with middle valued λ.

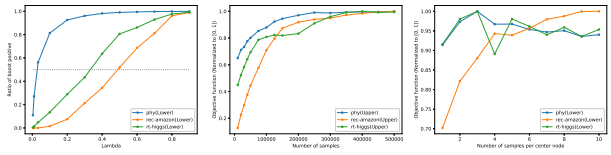

(a) Ratio of boosted C_a (b) Upper bound value (c) Lower bound value

Figure 7: SA-IMM test with λ and sample size varying

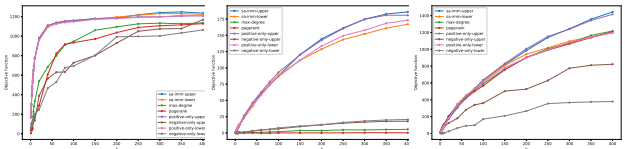

(a) Phy($\lambda = 0.275$) (b) rec-Amazon($\lambda = 0.9$) (c) rt-Higgs($\lambda = 0.9$)

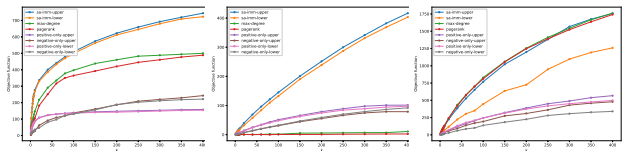

(d) Phy($\lambda = 0.0275$) (e) rec-Amazon($\lambda = 0.5$) (f) rt-Higgs($\lambda = 0.33$)

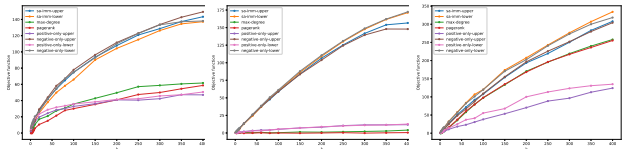

(g) Phy($\lambda = 0.00275$) (h) rec-Amazon($\lambda = 0.05$) (i) rt-Higgs($\lambda = 0.033$)

Figure 8: SA-IMM with Different λ Value (k Varying).

6.4 Results of SA-RG-IMM under nM-nS case

6.4.1 Test by varying λ and sample size. The affection of parameter λ and sample size in Fig.10, as observed, are very similar to that in Fig.7. Note in Fig.9(b) and (c), we set $\lambda = 0.03$ for Phy, 0.475 for rec-Amazon and 0.275 for rt-Higgs respectively. In the following, we fix the sample number of upper bound optimization to 150K and for lower bound optimization to 5 per node.

6.4.2 Performance with different λ. For each datasets, we set three different λ value to further observe the performance with assistant set size k varied. The results are shown in Fig.10. We can see the upper and lower bound version of SA-RG-IMM are outperforming in all the cases. Meanwhile, the upper bound version always outperforms the lower bound version. The priority we used is $C_a^+ \succ C_r^- \succ C_a \succ C_r$, which is quite similar to the upper bound priority $C_a^+ \succ C_r^- \succ C_r \succ C_a$. Thus the outperforming of the upper

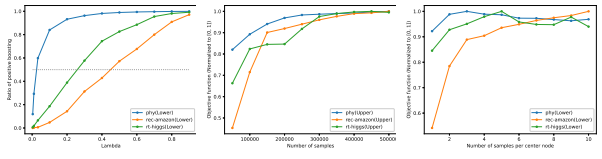

(a) Ratio of boosted C_a (b) Upper bound value (c) Lower bound value

Figure 9: SA-RG-IMM test with λ and sample size varying

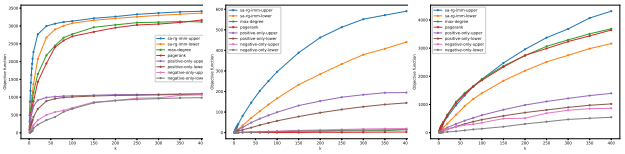

(a) Phy($\lambda = 0.25$) (b) rec-Amazon($\lambda = 0.9$) (c) rt-Higgs($\lambda = 0.9$)

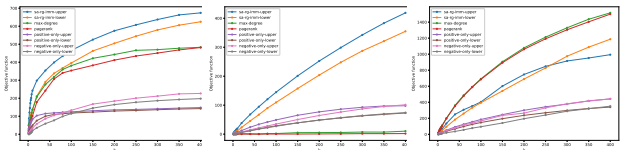

(d) Phy($\lambda = 0.03$) (e) rec-Amazon($\lambda = 0.5$) (f) rt-Higgs($\lambda = 0.275$)

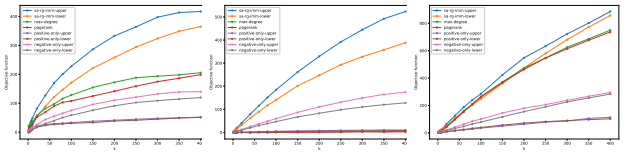

(g) Phy($\lambda = 0.0025$) (h) rec-Amazon($\lambda = 0.05$) (i) rt-Higgs($\lambda = 0.025$)

Figure 10: SA-RG-IMM with Different λ Value (k Varying).

bound version is within expectation. In addition, except the case in Fig.10(f), the performance of SA-RG-IMM methods are much more outperforming than the comparisons. This demonstrates the effectiveness of the propose algorithms. While the case of middle valued λ in Fig.10(f), where SA-RG-IMM methods perform poorly, is due to the same reason analyzed as Fig.8(f).

To conclude, the upper and lower bound optimization of SA-IMM and SA-RG-IMM are practical for dealing with variety of influence control applications, by tuning λ flexibly.

6.5 Time and Memory Usage

We also conduct experiments to show the time and memory usage of the SA-IMM and SA-RG-IMM algorithms, along with the sample number changing. The results are shown in Fig.11 and 12. We can see the time usage are consistent to the expectation, i.e., linear to the sample size. The rt-higg is the largest dataset with the largest time usage. The phy is the second time consuming since it is denser than rec-amazon while the size of these two datasets are close. The memory usage of rt-higg and rec-amazon are stable while of phy increases fast with sample number being large. This is because phy has the largest density. It costs much higher auxiliary space ($O(EPT^2)$), where EPT is the expected size of a single

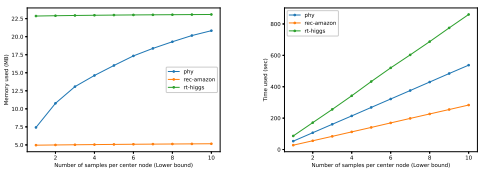

(a) Memory of lower bound (b) Runtime of lower bound

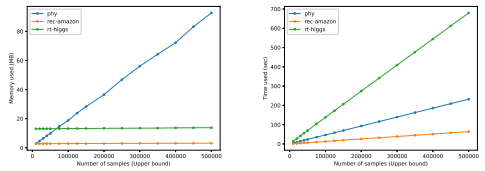

(c) Memory of upper bound (d) Runtime of upper bound

Figure 11: Time and Memory of SA-IMM.

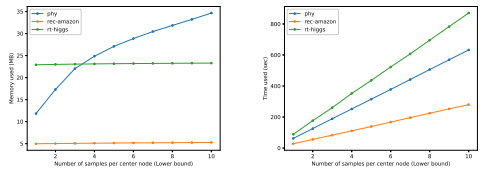

(a) Memory of lower bound (b) Runtime of lower bound

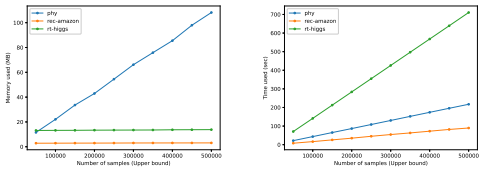

(c) Memory of upper bound (d) Runtime of upper bound

Figure 12: Time and Memory of SA-RG-IMM.

sample. Nevertheless, we can conclude that by setting an appropriate sample number achieve satisfactory performance with bearable time and memory usage. In this paper, the running time of all the proposed algorithms are not longer than 10 minutes, using the memory not larger than 50MB. These results show the time and memory effectiveness of the proposed algorithms in real world applications.

7 CONCLUSION AND FUTURE WORKS

In this paper, we propose the C^{2}IC model which generalize three well-known influence spread models. We analyze the corresponding C^{2}IM problem and design 4 algorithms according to the M&S case classification of different priorities. Both theoretically and experimentally, we show the effectiveness of the propose algorithms. Now we discuss some future works. First, a more in-depth relation between priority and M&S holding conditions are expected to be explored. Second, a more general and unified model that can describe the multi-agent multi-campaign influence spread scenarios, is expected to be constructed. It is worthy trying to streamline the research works in this area.

REFERENCES

[1] Cigdem Aslay, Wei Lu, Francesco Bonchi, Amit Goyal, and Laks V. S. Lakshmanan. 2015. Viral Marketing Meets Social Advertising: Ad Allocation with Minimum Regret. *Proc. VLDB Endow.* 8, 7 (feb 2015), 814–825.

[2] N. Barbieri, F. Bonchi, and G. Manco. 2012. Topic-Aware Social Influence Propagation Models. In *International Conference on Data Mining*.

[3] Shishir Bharathi, David Kempe, and Mahyar Salek. 2007. Competitive Influence Maximization in Social Networks. In *Internet and Network Economics*, Xiaotie Deng and Fan Chung Graham (Eds.). Springer Berlin Heidelberg, Berlin, Heidelberg, 306–311.

[4] Allan Borodin, Yuval Filmus, and Joel Oren. 2010. Threshold Models for Competitive Influence in Social Networks. In *Internet and Network Economics*, Amin Saberi (Ed.). Springer Berlin Heidelberg, Berlin, Heidelberg, 539–550.

[5] Niv Buchbinder, Moran Feldman, Joseph Naor, and Roy Schwartz. 2014. Submodular maximization with cardinality constraints. In *Proceedings of the twenty-fifth annual ACM-SIAM symposium on Discrete algorithms*. SIAM, 1433–1452.

[6] Ceren Budak, Divyakant Agrawal, and Amr El Abbadi. 2011. Limiting the Spread of Misinformation in Social Networks. In *Proceedings of the 20th International Conference on World Wide Web* (Hyderabad, India) *(WWW '11)*. Association for Computing Machinery, New York, NY, USA, 665–674.

[7] Ceren Budak, Divyakant Agrawal, and Amr El Abbadi. 2011. Limiting the spread of misinformation in social networks. In *Proceedings of the 20th international conference on World wide web*. ACM, 665–674.

[8] Deepayan Chakrabarti, Yang Wang, Chenxi Wang, Jurij Leskovec, and Christos Faloutsos. 2008. Epidemic Thresholds in Real Networks. *ACM Trans. Inf. Syst. Secur.* 10, 4, Article 1 (jan 2008), 26 pages.

[9] Shuo Chen, Ju Fan, Guoliang Li, Jianhua Feng, Kian-lee Tan, and Jinhui Tang. 2015. Online Topic-Aware Influence Maximization. *Proc. VLDB Endow.* 8, 6 (feb 2015), 666–677. https://doi.org/10.14778/2735703.2735706

[10] Wei Chen, Alex Collins, Rachel Cummings, Te Ke, Zhenming Liu, David Rincon, Xiaorui Sun, Yajun Wang, Wei Wei, and Yifei Yuan. [n.d.]. *Influence Maximization in Social Networks When Negative Opinions May Emerge and Propagate*. 379–390. https://doi.org/10.1137/1.9781611972818.33

[11] Wei Chen, Alex Collins, Rachel Cummings, Te Ke, Zhenming Liu, David Rincon, Xiaorui Sun, Yajun Wang, Wei Wei, and Yifei Yuan. 2011. Influence maximization in social networks when negative opinions may emerge and propagate. In *Proceedings of the 2011 siam international conference on data mining*. SIAM, 379–390.

[12] Wei Chen, Laks V.S. Lakshmanan, and Carlos Castillo. 2013. Information and Influence Propagation in Social Networks. *Synthesis Lectures on Data Management* 5, 4 (2013), 1–177. https://doi.org/10.2200/S00527ED1V01Y201308DTM037

[13] Wei Chen, Wei Lu, and Ning Zhang. 2012. Time-Critical Influence Maximization in Social Networks with Time-Delayed Diffusion Process. *Proceedings of the AAAI Conference on Artificial Intelligence* 26, 1 (Sep. 2012), 591–598.

[14] Wei Chen, Chi Wang, and Yajun Wang. 2010. Scalable influence maximization for prevalent viral marketing in large-scale social networks. In *Proceedings of the 16th ACM SIGKDD international conference on Knowledge discovery and data mining*. ACM, 1029–1038.

[15] Sainyam Galhotra, Akhil Arora, and Shourya Roy. 2016. Holistic Influence Maximization: Combining Scalability and Efficiency with Opinion-Aware Models. In *Proceedings of the 2016 International Conference on Management of Data* (San Francisco, California, USA) *(SIGMOD '16)*. Association for Computing Machinery, New York, NY, USA, 743–758.

[16] Manuel Gomez-Rodriguez, Le Song, Nan Du, Hongyuan Zha, and Bernhard Schölkopf. 2016. Influence Estimation and Maximization in Continuous-Time Diffusion Networks. *ACM Trans. Inf. Syst.* 34, 2, Article 9 (feb 2016), 33 pages.

[17] Xinran He, Guojie Song, Wei Chen, and Qingye Jiang. [n.d.]. *Influence Blocking Maximization in Social Networks under the Competitive Linear Threshold Model*. 463–474. https://doi.org/10.1137/1.9781611972825.40

[18] David Kempe, Jon Kleinberg, and Éva Tardos. 2003. Maximizing the spread of influence through a social network. In *Proceedings of the ninth ACM SIGKDD international conference on Knowledge discovery and data mining*. ACM, 137–146.

[19] Elias Boutros Khalil, Bistra Dilkina, and Le Song. 2014. Scalable diffusion-aware optimization of network topology. In *Proceedings of the 20th ACM SIGKDD international conference on Knowledge discovery and data mining*. ACM, 1226–1235.

[20] Guoliang Li, Shuo Chen, Jianhua Feng, Kian-lee Tan, and Wen-syan Li. 2014. Efficient Location-Aware Influence Maximization. In *Proceedings of the 2014 ACM SIGMOD International Conference on Management of Data* (Snowbird, Utah, USA) *(SIGMOD '14)*. Association for Computing Machinery, New York, NY, USA, 87–98.

[21] Hui Li, Sourav S. Bhowmick, Jiangtao Cui, Yunjun Gao, and Jianfeng Ma. 2015. GetReal: Towards Realistic Selection of Influence Maximization Strategies in Competitive Networks. In *Proceedings of the 2015 ACM SIGMOD International Conference on Management of Data* (Melbourne, Victoria, Australia) *(SIGMOD '15)*. Association for Computing Machinery, New York, NY, USA, 1525–1537. https://doi.org/10.1145/2723372.2723710

[22] Yishi Lin, Wei Chen, and John C.S. Lui. 2017. Boosting Information Spread: An Algorithmic Approach. In *2017 IEEE 33rd International Conference on Data Engineering (ICDE)*. 883–894. https://doi.org/10.1109/ICDE.2017.137

[23] Yishi Lin, Wei Chen, and John CS Lui. 2017. Boosting information spread: An algorithmic approach. In *Data Engineering (ICDE), 2017 IEEE 33rd International Conference on*. IEEE, 883–894.

[24] Wei Lu, Wei Chen, and Laks VS Lakshmanan. 2015. From competition to complementarity: comparative influence diffusion and maximization. *Proceedings of the VLDB Endowment* 9, 2 (2015), 60–71.

[25] Wei Lu, Wei Chen, and Laks V. S. Lakshmanan. 2015. From Competition to Complementarity: Comparative Influence Diffusion and Maximization. *Proc. VLDB Endow.* 9, 2 (oct 2015), 60–71.

[26] Seth A. Myers and Jure Leskovec. 2012. Clash of the Contagions: Cooperation and Competition in Information Diffusion. In *2012 IEEE 12th International Conference on Data Mining*. 539–548. https://doi.org/10.1109/ICDM.2012.159

[27] Ramasuri Narayanam and Amit A. Nanavati. 2012. Viral Marketing for Product Cross-Sell through Social Networks. In *Machine Learning and Knowledge Discovery in Databases*, Peter A. Flach, Tijl De Bie, and Nello Cristianini (Eds.). Springer Berlin Heidelberg, Berlin, Heidelberg, 581–596.

[28] Matthew Richardson and Pedro Domingos. 2002. Mining knowledge-sharing sites for viral marketing. In *Proceedings of the eighth ACM SIGKDD international conference on Knowledge discovery and data mining*. ACM, 61–70.

[29] Ryan A. Rossi and Nesreen K. Ahmed. 2015. The Network Data Repository with Interactive Graph Analytics and Visualization. In *AAAI*. https://networkrepository.com

[30] Muhammad Aamir Saleem, Rohit Kumar, Toon Calders, Xike Xie, and Torben Bach Pedersen. 2017. Location Influence in Location-Based Social Networks. In *Proceedings of the Tenth ACM International Conference on Web Search and Data Mining* (Cambridge, United Kingdom) *(WSDM '17)*. Association for Computing Machinery, New York, NY, USA, 621–630. https://doi.org/10.1145/3018661.3018705

[31] Qihao Shi, Can Wang, Jiawei Chen, Yan Feng, and Chun Chen. 2019. Location driven influence maximization: Online spread via offline deployment. *Knowledge-Based Systems* 166 (2019), 30–41. https://doi.org/10.1016/j.knosys.2018.12.003

[32] Qihao Shi, Can Wang, Jiawei Chen, Yan Feng, and Chun Chen. 2019. Post and repost: A holistic view of budgeted influence maximization. *Neurocomputing* 338 (2019), 92–100. https://doi.org/10.1016/j.neucom.2019.02.010

[33] Qihao Shi, Can Wang, Deshi Ye, Jiawei Chen, Yan Feng, and Chun Chen. 2019. Adaptive Influence Blocking: Minimizing the Negative Spread by Observation-Based Policies. In *2019 IEEE 35th International Conference on Data Engineering (ICDE)*. 1502–1513. https://doi.org/10.1109/ICDE.2019.00135

[34] Qihao Shi, Can Wang, Deshi Ye, Jiawei Chen, Sheng Zhou, Yan Feng, Chun Chen, and Yanhao Huang. 2021. Profit maximization for competitive social advertising. *Theoretical Computer Science* 868 (2021), 12–29. https://doi.org/10.1016/j.tcs.2021.03.036

[35] Lichao Sun, Weiran Huang, Philip S. Yu, and Wei Chen. 2018. Multi-Round Influence Maximization. In *Proceedings of the 24th ACM SIGKDD International Conference on Knowledge Discovery & Data Mining* (London, United Kingdom) *(KDD '18)*. Association for Computing Machinery, New York, NY, USA, 2249–2258.

[36] Jing Tang, Xueyan Tang, and Junsong Yuan. 2018. Profit Maximization for Viral Marketing in Online Social Networks: Algorithms and Analysis. *IEEE Transactions on Knowledge and Data Engineering* 30, 6 (2018), 1095–1108. https://doi.org/10.1109/TKDE.2017.2787757

[37] Youze Tang, Yanchen Shi, and Xiaokui Xiao. 2015. Influence maximization in near-linear time: a martingale approach. In *Proceedings of the 2015 ACM SIGMOD International Conference on Management of Data*. ACM, 1539–1554.

[38] Youze Tang, Xiaokui Xiao, and Yanchen Shi. 2014. Influence maximization: Near-optimal time complexity meets practical efficiency. In *Proceedings of the 2014 ACM SIGMOD international conference on Management of data*. ACM, 75–86.

[39] Amo Tong, Ding-Zhu Du, and Weili Wu. 2018. On Misinformation Containment in Online Social Networks. In *Advances in Neural Information Processing Systems*, S. Bengio, H. Wallach, H. Larochelle, K. Grauman, N. Cesa-Bianchi, and R. Garnett (Eds.), Vol. 31. Curran Associates, Inc.

[40] Guangmo Tong, Weili Wu, Ling Guo, Deying Li, Cong Liu, Bin Liu, and Ding-Zhu Du. 2020. An Efficient Randomized Algorithm for Rumor Blocking in Online Social Networks. *IEEE Transactions on Network Science and Engineering* 7, 2 (2020), 845–854. https://doi.org/10.1109/TNSE.2017.2783190

[41] Guangmo Tong, Weili Wu, Shaojie Tang, and Ding-Zhu Du. 2017. Adaptive Influence Maximization in Dynamic Social Networks. *IEEE/ACM Transactions on Networking* 25, 1 (2017), 112–125. https://doi.org/10.1109/TNET.2016.2563397

[42] Vijay V Vazirani. 2013. *Approximation algorithms*. Springer Science & Business Media.

[43] Ruidong Yan, Yi Li, Weili Wu, Deying Li, and Yongcai Wang. 2019. Rumor blocking through online link deletion on social networks. *ACM Transactions on Knowledge Discovery from Data (TKDD)* 13, 2 (2019), 1–26.

[44] Jing Yuan and Shaojie Tang. 2017. No Time to Observe: Adaptive Influence Maximization with Partial Feedback. In *Proceedings of the 26th International Joint Conference on Artificial Intelligence* (Melbourne, Australia) *(IJCAI'17)*. AAAI Press, 3908–3914.

[45] Yuqing Zhu, Deying Li, and Zhao Zhang. 2016. Minimum cost seed set for competitive social influence. In *IEEE INFOCOM 2016 - The 35th Annual IEEE International Conference on Computer Communications*. 1–9. https://doi.org/10.1109/INFOCOM.2016.7524472